Geotextiles and Geomembranes 46 (2018) 111–120

Contents lists available at ScienceDirect

Geotextiles and Geomembranes

journal homepage: www.elsevier.com/locate/geotexmem

Strain distribution along geogrid-reinforced asphalt overlays under traffic loading

N.S. Correia[a,*], J.G. Zornberg[b]

[a] Federal University of Sao Carlos, Department of Civil Engineering, Washington Luis Road (SP-310), Km 235, 13566-536, Sao Carlos, SP, Brazil
[b] The University of Texas at Austin, Civil Engineering Department, University Station C1792 Austin, TX 78712-0280, USA

ARTICLE INFO

Keywords:
Geosynthetics
Geogrid
Asphalt overlay
Reinforcement mechanism
Strain distribution

ABSTRACT

While there is significant field evidence of the benefits of geosynthetic-reinforced asphalt overlays, their use has focused on minimizing the development of reflective cracks. Yet, geogrids in asphalt overlays are also expected to develop reinforcement mechanisms that contribute to the pavement structural capacity. Specifically, the use of geosynthetics in asphalt overlays may also improve the mechanical behavior of paved roads by controlling permanent displacements and reducing strains in the pavement layers. While relevant advances have been made towards identifying the mechanisms in geosynthetic stabilization of base courses, such mechanisms may differ from those that develop in geosynthetic-reinforced asphalt overlays. This paper investigates the development and distribution of tensile strains along geogrids used to reinforce asphaltic layers. Experimental data was collected from large-scale paved road models subjected to the repeated loading imparted by wheel traffic. Specifically, the study examines both the elastic and permanent components of displacements induced in geogrids by using mechanical extensometers attached to the geogrids. The testing program includes a number of geosynthetic-reinforced paved road models, as well as a control (unreinforced) section that was also instrumented for comparison purposes. Asphalt strain gauges were used to measure strains within the asphalt concrete layer, providing an additional source of information that proved to be highly consistent with the results obtained from the extensometers. The experimental results showed a progressive mobilization of permanent geogrid strains that reached a final profile beyond which additional traffic loading did not result in additional straining. In comparison, higher strains developed in the unreinforced model, which showed a continuously increasing trend. Elastic tensile strains in the asphalt mixture and rutting under the wheel load were comparatively smaller when using geogrids. Overall, the results generated in this study indicate that the presence of geogrids in asphalt overlays results in a lateral restraining mechanism that influences on the mechanical behavior of flexible pavements.

1. Introduction

Significant evidence has been reported regarding the benefits of geosynthetic-reinforced asphalt overlays to minimize the development of reflective cracks (Fallah and Khodaii, 2015; Gonzalez-Torre et al., 2015; Nejad et al., 2016), which has been primarily use of this technique. Yet, evidence has also been preliminarily identified that suggests that geogrids could develop reinforcement mechanisms that may lead to an increased pavement structural capacity. Specifically, the use of geosynthetics in asphalt overlays may also improve the mechanical behavior of paved roads by controlling permanent displacements and reducing strains in the pavement layers (Laurinavicius and Oginskas, 2006; Siriwardane et al., 2010; Solaimanian, 2013; Graziani et al., 2014; Mounes et al., 2015; Correia and Zornberg, 2016).

Relevant advances have been made towards understanding the mechanisms that lead to stabilization of base aggregates and subgrade layers using geosynthetics (e.g. Perkins and Ismeik, 1997; Holtz et al., 1998; USACOE, 2003). While relevant advances have been made towards identifying the mechanisms that develop in geosynthetic-stabilized base and subgrade layers, they may differ from those that develop in geosynthetic-reinforced asphalt overlays (Correia and Zornberg, 2016; Zornberg, 2017a, 2017b).

Using large-scale paved road models, Perkins (1999) investigated the pattern of tensile strains that develop in geogrid-reinforced bases under dynamic plate load testing. Evidence of the development of lateral restraint mechanisms in the base layer was identified through the measurement of geosynthetic tensile strains. Abu-Farsakh et al. (2011) conducted an additional investigation on the development and

---

[*] Corresponding author.
E-mail addresses: ncorreia@ufscar.br (N.S. Correia), zornberg@mail.utexas.edu (J.G. Zornberg).

http://dx.doi.org/10.1016/j.geotexmem.2017.10.002
Received 25 January 2017; Received in revised form 20 September 2017; Accepted 8 October 2017

distribution of tensile strains along geogrids in base stabilization applications. Permanent tensile strains were found to develop along the geogrids, which were attributed to the development of tension that restrains lateral movements within the base course aggregate.

Ling and Liu (2001) conducted full-scale monotonic and dynamic loading tests to monitor the strain distribution along geogrids installed at the bottom of asphalt concrete layers, along the asphalt-subgrade interface. Geogrid strains were recorded using strain gauges placed at different locations along the geogrid. The restraining effect of geogrids was quantified by monitoring the strains that developed in the vicinity of the loading area.

A comparatively smaller number of studies has been conducted to evaluate the development of geogrid strains for cases involving the reinforcement of asphaltic layers under traffic loading. A study identified for this application is that conducted by Nguyen et al. (2013), although the focus of the investigation was on the use of glass-fiber reinforcements rather than polymeric geogrids. The study presented the results from an accelerated pavement testing field program where glass-fiber reinforcement was installed between two new asphaltic layers placed on an existing pavement structure. The geogrid was instrumented with strain gauges and positioned under the center of one-wheel and dual-wheel load systems. Although monitoring data indicated no significant reduction of strains in the geogrid-reinforced section (longitudinal direction of the wheel track), the study demonstrated the relevance of measuring the development of strains and strain distribution that develop in geogrid reinforcements embedded in asphaltic layers. Unfortunately, no studies were identified that report on the development of geogrid strains in reinforced asphalt overlays under traffic loading.

In summary, a review of previous studies involving the reinforcement of asphaltic layers reveals that only limited information is currently available to assess the impact of the geogrids on enhancing the roadway structural capacity. In particular, information is lacking regarding the possible mechanisms that could lead to an improved long-term behavior of geogrid-reinforced asphalt layers. Consequently, this paper focuses on investigating the development of tensile strains along geogrids placed within the asphaltic layers of full-scale paved road models subjected to wheel loading. The study quantifies and evaluates the mobilized elastic and permanent geogrid displacements, measured using mechanical extensometers attached to geogrid layers. This information facilitates the understanding of the pavement response and is expected to lead to the development of methodologies to predict the response of asphalt-reinforced pavements. The testing program includes geosynthetic-reinforced paved road models, as well as a control (unreinforced) section that was also instrumented for comparative purposes.

2. Overview of the experimental setup

A brief description of the wheel tracking facility used in this study, the scope of the experimental program and the instrumentation plan used in the research program are presented in this section. Additional description of the test wheel facility and scope of the experimental testing program is provided by Correia and Zornberg (2016).

2.1. Wheel tracking facility

The large-scale paved road models constructed as part of this study were loaded using a wheel tracking facility that aimed at simulating the moving load of a truck wheel. The wheel tracking facility was installed in a comparatively large steel testing box with internal dimensions of 1.8 m (height), 1.6 m (width) and 1.8 m (length). Fig. 1 shows a view of the wheel tracking facility. The wheel moves at a speed of 3.6 km/h in contact with a 1 m-long tracking path. It involves a tire wheel characterized by a diameter of 546 mm and a width of 154 mm, which applied a contact pressure of approximately 700 kPa. A total of 10^5 passes was applied in each test in a unidirectional mode at a wheel load pulse frequency of 0.4 Hz. Correia and Zornberg (2016) provide additional details on the cyclic load pulses used in this research. The different layers in the paved road system included a silty clay subgrade soil, a granular base and a hot mix asphalt concrete layer.

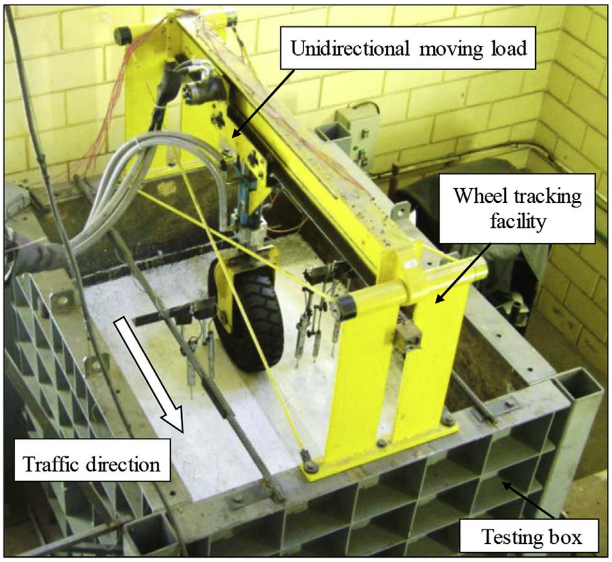

Fig. 1. View of the wheel tracking facility.

2.2. Paved road materials and layer characteristics

The classification and mechanical properties of the different materials used to construct the large-scale paved road models are summarized in Table 1. This includes the characteristics of the subgrade soil, base aggregate and asphalt concrete mix. The subgrade soil was compacted in the testing box in 50 mm-thick lifts using manual procedures that involved a drop hammer. The selected target dry density and water content used during construction resulted in a relatively weak subgrade, characterized by a California Bearing Ratio (CBR) of 4.5%. The

Table 1
Properties of the materials used during construction of the paved road models.

Property	Test method	Value
Subgrade soil		
USCS Classification	(ASTM D2487-11)	ML
AASHTO Classification	(AASHTO M 145-91)	A-7-5
Maximum dry density	Standard Proctor Compaction (ASTM D698-12e2)	14.9 kN/m^2
Target dry density for compaction		14.7 kN/m^2
Compaction water content		30.8% (2% above optimum)
CBR using target compaction values	California bearing ratio (ASTM D1883-14)	4.5%
Base aggregate material		
USCS Classification	(ASTM D2487-11)	**GP**
AASHTO Classification	(AASHTO M 145-91)	**A-1-a**
Maximum dry density	Standard Proctor Compaction (ASTM D698-12e2)	24 kN/m^3
Optimum moisture content		6.5%
Relative compaction (as compacted)		99%
Hot mix asphalt concrete (as compacted)		
Strength of Bituminous Mixtures	Indirect tensile strength (ASTM D6931-07)	1.0 MPa
Resilient Modulus - Asphaltic layer	Repeated-load indirect tension test	3500 MPa
Resilient Modulus - Asphalt overlay	(ASTM D7369-11)	4500 MPa